

# Liquid phase assisted densification of superhard B<sub>6</sub>O materials

Mathias Herrmann<sup>a,\*</sup>, Jan Raethel<sup>a</sup>, Axel Bales<sup>a</sup>, Kerstin Sempf<sup>a</sup>,  
Iakovos Sigalas<sup>b</sup>, Mandy Hoehn<sup>a</sup>

<sup>a</sup> *Fraunhofer Institute for Ceramic Technologies and Systems, D01640 Dresden, Germany*

<sup>b</sup> *School of Chemical and Metallurgical Engineering, University of the Witwatersrand, Johannesburg, South Africa*

Received 19 December 2008; received in revised form 2 March 2009; accepted 5 March 2009

Available online 5 April 2009

## Abstract

B<sub>6</sub>O-based materials are known as some of the hardest materials after diamond and cubic boron nitride with a hardness of 45 GPa measured on single crystals. Several attempts were made to produce B<sub>6</sub>O materials by hot pressing, but without success. Based on thermodynamic considerations the possibility of the use of sintering additives was discussed and the developed concepts were validated by densification of the materials using FAST (field assisted sintering technique)/SPS methods and analysing the microstructure and properties of the resulting materials. Two groups of materials were found to be suitable for the densification: transition metals which form borides with B<sub>6</sub>O, the elements of the first to fourth main groups of the periodic table and the rare earths (Sc, Y, and lanthanides) which are in equilibrium in the oxide form with B<sub>6</sub>O and form a liquid phase during densification at 1700–1900 °C. Superhard dense B<sub>6</sub>O materials were produced and their properties investigated.

© 2009 Elsevier Ltd. All rights reserved.

**Keywords:** Sintering; Microstructure-final; Hardness; Borides

## 1. Introduction

B<sub>6</sub>O-based materials are known as some of the hardest materials after diamond and cubic boron nitride with a hardness of 45 GPa measured on single crystals.<sup>1</sup> The structure of B<sub>6</sub>O is quite similar to the structure of B<sub>4</sub>C but B<sub>6</sub>O is even harder than B<sub>4</sub>C.<sup>2</sup> However, these materials have not been used in commercial applications so far because of the requirement to use high pressure (1–5 GPa) in order to achieve fully dense materials.<sup>3</sup> The resulting materials had good hardness but very low fracture toughness (1–2 MPa m<sup>1/2</sup>).<sup>3</sup> B<sub>6</sub>O consists of B<sub>12</sub> icosahedral units connected by covalent bonds. Like B<sub>4</sub>C, B<sub>6</sub>O can be nonstoichiometric. It has the overall formula B<sub>6</sub>O<sub>1-x</sub> with  $x$  between 1 and 0.72. The high  $x$  values, i.e. the stoichiometric composition, were observed only in compounds made under high pressure synthesis.<sup>4,5</sup>

Efforts were made to enhance the mechanical properties of B<sub>6</sub>O, especially its fracture toughness, by forming B<sub>6</sub>O compos-

ites with other hard materials such as diamond,<sup>6</sup> boron carbide<sup>7</sup> and cBN.<sup>8</sup> Even though high hardness values were recorded for the composites ( $H_V \sim 46$  GPa), again, fracture toughness values did not exceed 1.8 MPa m<sup>1/2</sup>.<sup>6,8</sup>

B<sub>6</sub>O materials were prepared by hot pressing mixtures of B and B<sub>2</sub>O<sub>3</sub> at temperatures up to 2000 °C.<sup>9,10</sup> These materials had high microhardness, but no other mechanical properties were determined. Hot pressing of B<sub>6</sub>O powders in a wide temperature range described by Brodhag and Thévenot only resulted in porous materials with low hardness and poor mechanical properties.<sup>11</sup>

Recently we could show that B<sub>6</sub>O materials with the addition of Al<sub>2</sub>O<sub>3</sub> can be hot pressed at 1900 °C. The resulting materials have improved fracture toughness and only a slight reduction in hardness in comparison to pure B<sub>6</sub>O materials.<sup>12–14</sup> Microstructural analysis showed that aluminium borate is formed at the grain boundaries beside micropores. The investigation of the microstructure reveals that the material was densified, at least predominantly, by liquid phase sintering. The densification of B<sub>6</sub>O-materials at ambient pressure would make it possible to produce materials with properties similar to cBN-materials. The advantage of this method would be that no ultra high pressure is

\* Corresponding author. Fax: +49 3512553600.

E-mail address: [Mathias.Herrmann@ikts.fraunhofer.de](mailto:Mathias.Herrmann@ikts.fraunhofer.de) (M. Herrmann).

needed for the synthesis or the densification of these materials, as is the case for cBN materials.

The development of thermodynamic data for B<sub>6</sub>O at high temperatures<sup>13</sup> has allowed predictions of the stability of the different phases in B<sub>6</sub>O composites. On this basis several additives can be selected which could be suitable for the densification of B<sub>6</sub>O. This search for additives is of great importance for the reduction of sintering temperature and the tailoring of the microstructure. For successful liquid phase sintering, beside the formation and stability of a liquid phase, a wetting of the B<sub>6</sub>O by the main component is necessary. These data are difficult to predict and need experimental testing.

Based on thermodynamic calculations different groups of additive were determined and tested using FAST/SPS densification.

## 2. Experimental

The starting B<sub>6</sub>O powder was produced on a laboratory scale as described in literature.<sup>12</sup> The chemical composition of the B<sub>6</sub>O powder was determined using ICP OES. The compositions of the materials and the achieved properties are given in Table 1. The B<sub>6</sub>O starting powder contains 0.25% Al and 0.32% Mg. Beside B<sub>6</sub>O the following powders were used: Al<sub>2</sub>O<sub>3</sub> (AKP50, Sumitomo, Japan), Y<sub>2</sub>O<sub>3</sub> (Grade C, HC STARCK, Germany), TiB<sub>2</sub>, TiH<sub>2</sub> (Grade C, HC STARCK, Germany), ZrO<sub>2</sub> (Thoso, Japan), HfO<sub>2</sub> (Treibacher, Austria); WO<sub>3</sub> was produced from WC (HC STARCK, Germany) by oxidation at 650 °C 10 h, TiO<sub>2</sub> (P25, DEGUSSA, Germany). TiH<sub>2</sub> was used as Ti source because it can be better milled than Ti powder due to its brittleness and its decomposition at temperatures less than 1000 °C.

The powder was mixed in an attrition mill with alumina milling balls (1–2 mm, Al<sub>2</sub>O<sub>3</sub> 99.6%). The solvent was ethanol. After milling the suspension was dried using a rotation evaporator. The wear of the alumina balls (0.65%) was included in the overall composition of the materials in Table 1.

FAST/SPS was carried out on a HP D 25 furnace (FCT Company, Germany) using graphite dies with an inner diameter of

30 mm and graphite foils. The graphite foils were coated with a BN suspension to prevent the interaction with the graphite. The densification was carried out in Ar. The temperature was measured with a standard pyrometer in the centre of the die.

The heating rate was 50 K/min. Since a non-conductive hBN coating was used, the densification is rather a fast hot pressing than a classical SPS process, which is characterised by a current going through the powder.

The densification was monitored by measuring the piston travel. This measurement was then converted into relative density change, normalizing the end position of the piston during the isothermal holding to the measured final density of the sample. The piston travel contains a contribution from thermal expansion of the whole setup. The comparison of curves with dense samples showed that there is a relevant deviation only during application of the load.

Cross sections of the materials produced were polished. The prepared cross sections were analysed using FESEM (Leo 982) with attached EDX system. The phase composition was determined using XRD (XRD7, GE Inspection, Cu K $\alpha$ ).

For microhardness testing an MHT-10 apparatus with Vickers indenter from Anton Paar was used. The indenter was placed in a lens barrel of an Olympus microscope. The test force can be varied between 0.05 and 400 Pont. For the measurement of the indentation an Olympus microscope with 500-times magnification was used. The microhardness value was calculated by using the AnalySIS software. 10 s dwell time was used for the indentation at the highest load. Five indentations were made for every material and every load.

## 3. Results and discussion

### 3.1. Thermodynamic calculations

Using the thermodynamic data given in<sup>13</sup> and using the SGTE database as well as the FACTSAGE programm<sup>15</sup> the different oxides were studied to determine their stability in comparison

Table 1  
Properties of the densified B<sub>6</sub>O materials (heating rate 50 K/min, holding time at maximum temperature 5 min).

Material	Additives (wt%)	Pressure (MPa)	T (°C)	H <sub>V</sub> 0.4 (GPa)	Density (g/cm <sup>3</sup> )	Phases <sup>a</sup>
1	2.62 Al <sub>2</sub> O <sub>3</sub> , 2.65 Y <sub>2</sub> O <sub>3</sub>	50	1850	31.2 ± 0.6	2.56	B <sub>6</sub> O
1	2.62 Al <sub>2</sub> O <sub>3</sub> , 2.65 Y <sub>2</sub> O <sub>3</sub>	80	1800	33.0 ± 0.7	2.60	B <sub>6</sub> O
2(E) <sup>b</sup>	0	50	1900	34.2 ± 0.6	2.50	B <sub>6</sub> O
2(E) <sup>b</sup>	0	50	1850		2.36	B <sub>6</sub> O
5	2 Al <sub>2</sub> O <sub>3</sub> , 2 Y <sub>2</sub> O <sub>3</sub>	50	1850		2.53	B <sub>6</sub> O
5-ZrO <sub>2</sub>	2 Al <sub>2</sub> O <sub>3</sub> , 2 ZrO <sub>2</sub>	50	1900	36.9 ± 0.6	2.57	B <sub>6</sub> O, ZrB <sub>2</sub>
5b-ZrO <sub>2</sub>	2 Al <sub>2</sub> O <sub>3</sub> , 2 Y <sub>2</sub> O <sub>3</sub> , 2 ZrO <sub>2</sub>	50	1850		2.60	B <sub>6</sub> O, ZrB <sub>2</sub>
5b-HfO <sub>2</sub>	2 Al <sub>2</sub> O <sub>3</sub> , 2 Y <sub>2</sub> O <sub>3</sub> , 2 HfO <sub>2</sub>	50	1850		2.52	B <sub>6</sub> O, HfB <sub>2</sub>
5b-WO <sub>3</sub>	2 Al <sub>2</sub> O <sub>3</sub> , 2 Y <sub>2</sub> O <sub>3</sub> , 4 WO <sub>3</sub>	50	1850		2.61	B <sub>6</sub> O, W <sub>2</sub> B <sub>5</sub>
5-TiH <sub>2</sub>	2 Al <sub>2</sub> O <sub>3</sub> , 4 TiH <sub>2</sub>	50	1850	33.6 ± 0.6	2.51	B <sub>6</sub> O, TiB <sub>2</sub>
5-TiB <sub>2</sub>	2 Al <sub>2</sub> O <sub>3</sub>	50	1850		2.64	B <sub>6</sub> O, TiB <sub>2</sub>
	2 Y <sub>2</sub> O <sub>3</sub>					
	10 TiB <sub>2</sub>					
B + TiO <sub>2</sub>	B + TiO <sub>2</sub>	50	1900	36.8 ± 0.6	2.68	
		50	1850		2.79	B <sub>6</sub> O, TiB <sub>2</sub>

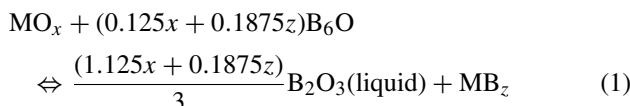
<sup>a</sup> Determined by XRD, an amorphous grain boundary is present.

<sup>b</sup> Pure B<sub>6</sub>O without additives.

to  $B_6O$ . A first approximation of the thermodynamic function of  $B_6O$  was obtained by McMillan.<sup>5</sup> The estimated value for  $\Delta H_{298}$  was  $-622.2$  kJ/mol. This is 20% less than the measured values ( $\Delta H_f^\theta(B_6O, 298.15\text{ K}) = -527 \pm 32$  kJ mol<sup>-1</sup>),<sup>20</sup> i.e. the measured data reveal a lower stability of  $B_6O$  than the estimated data of McMillan.<sup>5</sup> Calculations in this paper are based therefore on the measured values.<sup>20</sup>

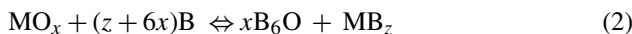
The interaction of  $B_6O$  with the different compounds could be described by two reactions:

- (1) The oxidation of  $B_6O$  and the formation of metals or borides. According to the reaction



If the Gibbs free energy of this reaction is positive, then the oxide is stable in contact with  $B_6O$ . It would also indicate that borides could react with  $B_2O_3$  and form  $B_6O$  giving the possibility to control the amount of  $B_2O_3$  in the starting powder.

- (2) It is important for the densification that  $MO_x$  can react with residual or added B in the starting powder and to form  $B_6O$ . This can also be an indication of the ability of the oxide to increase the oxygen content ( $x$  value) of the  $B_6O_{1-x}$  phase. This reaction can be formulated as follows:



Borides which are stable with  $B_6O$  must have a negative Gibbs free energy of reaction (2).

The Gibbs free energy of both reactions at 1700 °C, i.e. the desired sintering temperature is given in Fig. 1.

The formation of mixed compounds or liquids is not taken into account by the given thermodynamic data, because such data are not available for most of the oxides used in this study. The solubility of the different components in the liquid or the forma-

tion of mixed oxides or borates will slightly shift the boundary between the stable oxides and borides. This has to be taken into account. However, the  $\Delta G$  values of the reactions of the transition metal oxides with  $B_6O$  are quite negative, so that the equilibrium solubility of the oxides in the liquid/glass phase formed would be very small. Indeed no Ti, W, and Zr could be observed in the oxide triple junctions using EDX analysis (see Section 3.2).

The data show that all chosen transition metal oxides of the IV to the VIII group react with  $B_6O$  to form borides. All these oxides also oxidize B to  $B_6O$  (the  $\Delta G$  of reaction (2) is negative). This means that all the transition elements of these groups will form  $B_6O$ /boride composites independently of the starting powders (oxides + B or  $B_6O$ ;  $B_6O$  + metals or borides). Recent investigations of the interaction of Pd with  $B_6O$  revealed the formation of  $Pd_2B$ .<sup>16</sup> Thus, the formation of borides is also likely for the Pt-group elements.

A starting powder mixture of  $B_6O$  and the transition metal oxides will result in the formation of some additional  $B_2O_3$ . The addition of the oxides or the metals, therefore, can be used to control the overall oxygen content in the material. It has to be mentioned that  $B_2O_3$  has a high vapour pressure which could result in some decomposition of the materials.

All investigated oxides of the first to the fourth main group of the periodic table as well as the rare earths are in equilibrium with  $B_6O$  and can form an oxide secondary phase which forms a liquid during sintering interacting with some remaining  $B_2O_3$ . This was previously shown in the case of  $Al_2O_3$  addition.<sup>13,14</sup>

The Gibbs free energy of the reaction of the oxide with B (reaction (2)) is for some of the oxides negative, while for others it is positive. This would not restrict their use as sintering additives, but if boron is present in the starting powder or is produced by decomposition, then Si-, Al-...oxides will react with boron to form  $B_6O$  and borides. In the case of MgO additions the Mg rich borides can be formed. The  $\Delta G$  values of reaction (2) for La, Mg, and Li oxides are very close to 0. Therefore, the formation of stable mixed oxides or borides can shift the  $\Delta G$ .

On the basis of the calculations conducted in this work, an improved densification through liquid phase sintering can be expected using stable oxides like CaO,  $Y_2O_3$ ,  $Sc_2O_3$ , or other rare earths, or  $Al_2O_3$ ,  $SiO_2$ , and MgO, alone or in combination with each other. The use of alkaline oxides as sintering additives is restricted by their high vapour pressure.

The transition metal oxides used in this study can form only transient oxide liquid due to the interaction with the  $B_6O$  resulting in the formation of borides and some  $B_2O_3$  which forms a liquid, but has a high vapour pressure. The in situ formation of hard borides, e.g.  $TiB_2$ , offers the possibility to adapt the chemical composition or to use the metal oxide and B as a combined sintering additive.

To validate the thermodynamic findings different compositions of  $B_6O$  with  $Y_2O_3/Al_2O_3$ ,  $TiH_2$ ,  $TiB_2$ ,  $ZrO_2$ ,  $HfO_2$  and,  $WO_3$  additions were tested as sintering additives. The phase composition and some properties of the resulting materials were determined.

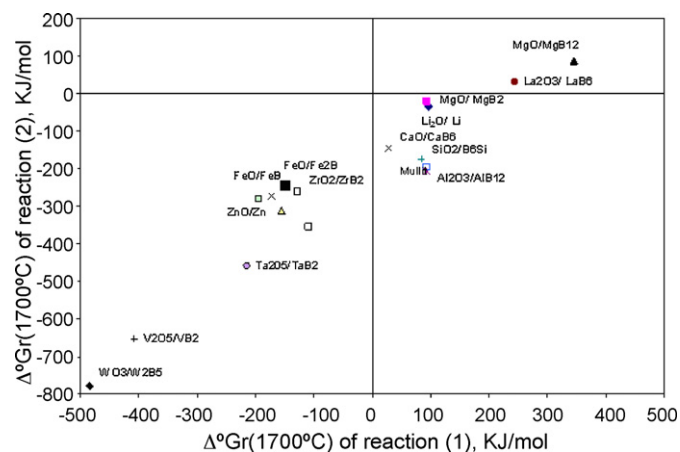


Fig. 1. Gibbs free energy of the interaction of different oxides with B and  $B_2O_3$  (The composition of the starting oxides and of the resulting boride/metal are marked at the points.).

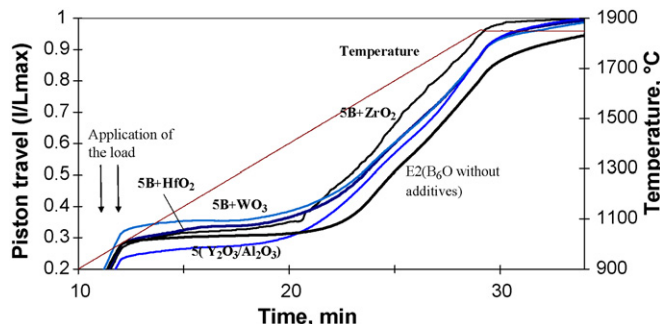


Fig. 2. Densification curves of the samples with different transition metal oxide additives in comparison to the pure  $B_6O$  powder and the material with  $Y_2O_3/Al_2O_3$  additives.

### 3.2. Densification and microstructure of the composites

The materials, densities, phase compositions and properties are given in Table 1. The densification curves are given in Figs. 2 and 3. The data showed that the addition of  $Y_2O_3/Al_2O_3$  strongly increases the degree of densification. Complete densification is achieved at  $1850^\circ C$  for the compositions with the additives, whereas the pure  $B_6O$  powders can only be densified to 95% of theoretical density at this temperature. The same density as for the pure material can be reached for materials with additives at temperatures which are 50–100 °C lower. Fast densification starts at 1350–1370 °C for the material with the  $Y_2O_3/Al_2O_3$  additives whereas the densification of the pure material starts only at  $1450^\circ C$  (Fig. 2).

Some  $B_2O_3$  is present on the surface of the  $B_6O$  powder as a result of the powder processing operation (approximately 1–1.5 wt%). This phase forms a liquid at temperatures above  $480^\circ C$  and allows the densification to occur at lower temperatures. At temperatures above 1700–1800 °C  $B_2O_3$  vigorously evaporates, and therefore the densification is retarded.<sup>6</sup> The added stable oxides  $Y_2O_3/Al_2O_3$  react with the  $B_2O_3$  and form a stable oxide rich liquid phase<sup>10</sup> during sintering which helps to reduce the densification temperature. The additives increase the amount of liquid and hinder the decomposition reactions during sintering in comparison to pure  $B_6O$  materials. Therefore, the addition of  $Y_2O_3/Al_2O_3$  (stable oxides) results in a more reproducible densification in comparison to pure  $B_6O$  materials.

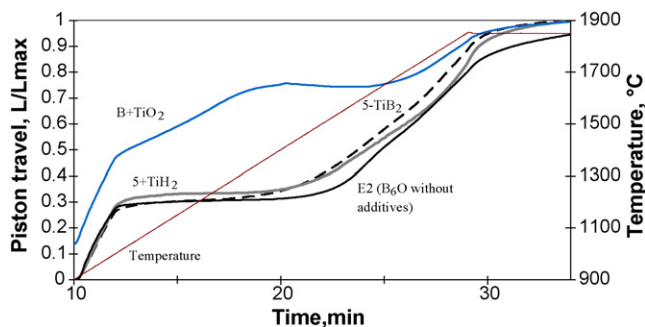


Fig. 3. Densification curves of the samples with different titanium containing additives in comparison to the pure  $B_6O$  powder and the material with  $Y_2O_3/Al_2O_3$  additives.

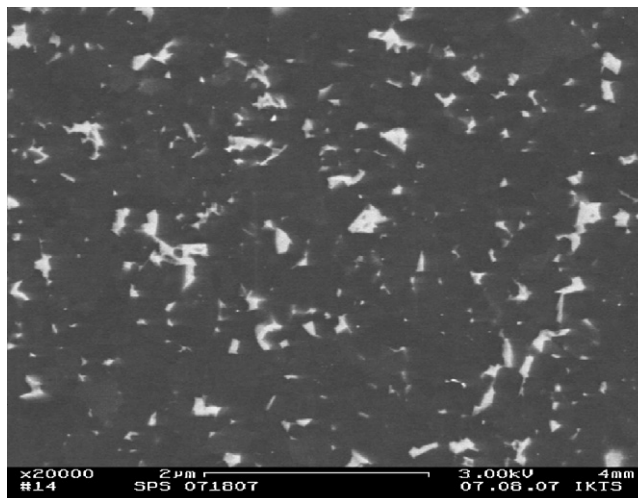


Fig. 4. SEM image of the microstructure of material 1.

The microstructures of the materials containing additives of  $Y_2O_3/Al_2O_3$  also reveal the presence of such a liquid, because no crystalline grain boundary phases are found. SEM micrographs in Fig. 4 shows a homogeneous distribution of the  $Y_2O_3/Al_2O_3$  additives (white phase) in the triple junctions.

The grain size of the material cannot be determined, but from the SEM micrographs it can be concluded that the grain size is less than  $1\ \mu m$ . Therefore, no grain growth occurs. This is most likely due to the very short sintering times employed (Fig. 4).

The addition of transition metal oxides also improves the densification in comparison to the pure  $B_6O$  powder. The increase in densification is not as pronounced as in the case of  $Y_2O_3/Al_2O_3$ .

At low temperatures the added transition metal oxides ( $ZrO_2$ ,  $TiO_2$ ,  $WO_3$ ) form a liquid with the  $B_2O_3$  present on the surface of the  $B_6O$  powder. The solubility of  $TiO_2$  or  $WO_3$  at  $1200^\circ C$  is 10–25 mol% (corresponding to 12–50 wt%, respectively).<sup>17</sup> Additionally, non-dissolved oxides can also remain in the resulting material. These remaining oxides can provide some lubricity because they can be densified at these temperatures.

The oxides are thermodynamically not stable (see Section 3.1) and quantitatively transform into borides and  $B_2O_3$  (reaction (1)). The  $B_2O_3$  decomposes, at least partially, at high temperatures.

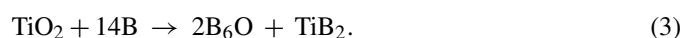
The borides formed have a high melting point and can only be sintered without additives at high temperatures.<sup>18</sup> Therefore, they cannot significantly accelerate the sintering in comparison to pure  $B_6O$ . At high temperatures, the remaining  $Al_2O_3$  and MgO (from the wear of the milling media and from the starting powder, respectively) only form a liquid with the  $B_2O_3$  improving the densification. Al, B, O and some Mg were found in the triple junctions examined by SEM/EDS (Fig. 6). The grain boundary pockets are partially removed by polishing indicating their lower chemical stability.

The grain boundary phase containing  $Y_2O_3/Al_2O_3$  is chemically much more stable than the boron rich grain boundary phase, which was observed in the materials containing the transition metal oxides and some  $Al_2O_3$ . The lower stability results in the partial removal of the grain boundary phases during polishing.

This becomes visible in Fig. 6b and is not visible in Fig. 4. From the investigations of borate glasses<sup>19</sup> it is known that the transition temperature of the amorphous grain boundary also increases up to 800 °C with Y<sub>2</sub>O<sub>3</sub>/Al<sub>2</sub>O<sub>3</sub> addition. This has a positive effect on the high temperature stability.

The conversion process of the transition metal oxides into borides takes place at temperatures below 1500–1600 °C. The completion of the reaction results in some retardation of the sintering at intermediate temperature. This is also clearly seen in the reaction sintering of B and TiO<sub>2</sub> (Fig. 3).

This mixture densifies much faster in the temperature region between 1000 and 1600 °C than the other composites with TiH<sub>2</sub> or TiB<sub>2</sub> additions. This is related to the reaction of TiO<sub>2</sub> with B:



A run interrupted at 1600 °C showed that TiB<sub>2</sub> and a very disturbed or nanocrystalline B<sub>6</sub>O are formed at these temperatures. However, the densification is only completed at temperatures higher than 1650 °C (Fig. 3).

The phase composition (B<sub>6</sub>O and TiB<sub>2</sub>) was found to be independent of the starting mixture (TiH<sub>2</sub> or TiB<sub>2</sub> + B<sub>6</sub>O or TiO<sub>2</sub> and B). As in the case of the phase composition of the other samples investigated in this work, this confirms the predictions of the thermodynamic calculations.

The addition of 10 wt% of TiB<sub>2</sub> to the composition of the B<sub>6</sub>O + Y<sub>2</sub>O<sub>3</sub>/Al<sub>2</sub>O<sub>3</sub> does not change the densification behaviour significantly (cf. curves in Figs. 2 and 3).

The microstructure of material 5-TiB<sub>2</sub> is shown in Fig. 5. It is possible by EDX analysis to see that the TiB<sub>2</sub> grains are in the range of 1–2 μm and that the oxide grain boundary contains Y<sub>2</sub>O<sub>3</sub>/Al<sub>2</sub>O<sub>3</sub> and some B<sub>2</sub>O<sub>3</sub>.

The microstructure of the materials with TiH<sub>2</sub> additions are given in Fig. 6. The material is dense and the formation of borides is visible. The particle size of the precipitated borides is less than 1 μm. During sample preparation the oxide grain boundary is more extensively removed by polishing than the hard B<sub>6</sub>O and borides. This more intensive polishing behaviour was observed only for the materials without Y<sub>2</sub>O<sub>3</sub> additions and with additions

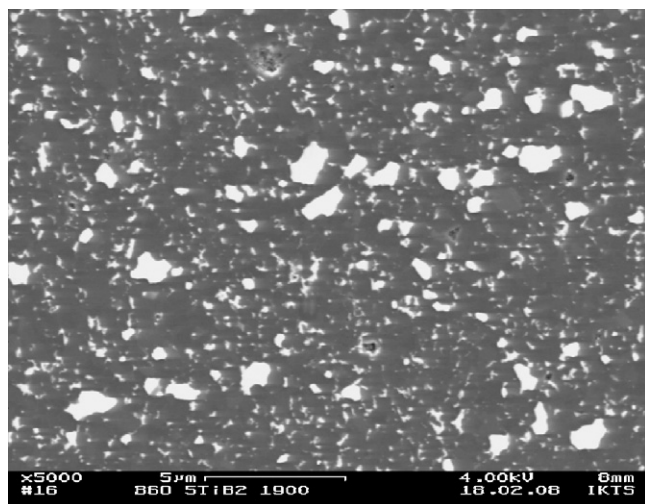


Fig. 5. SEM image of the microstructure of sample 5-TiB<sub>2</sub>.

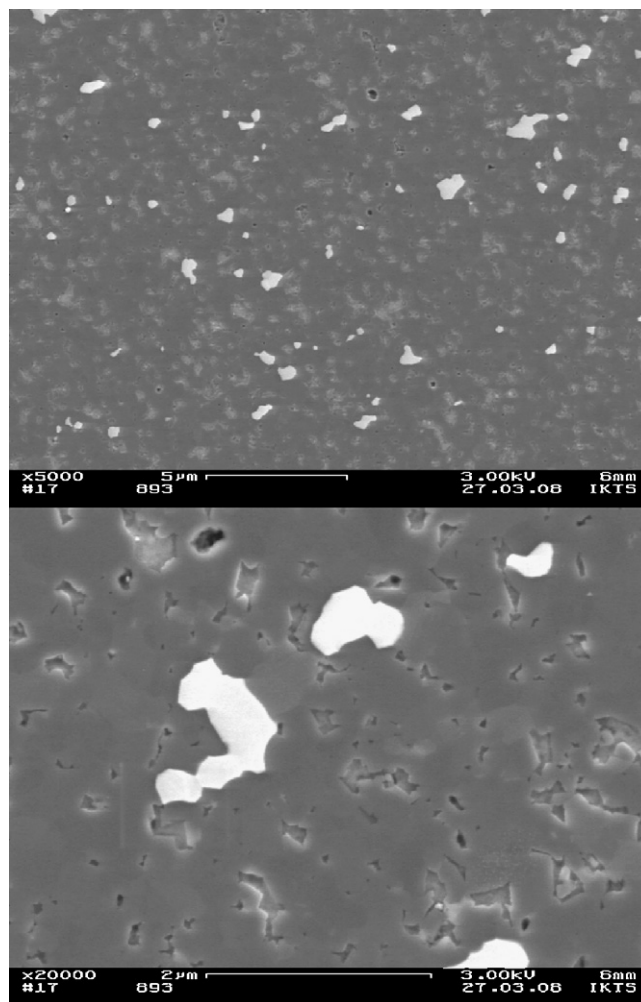
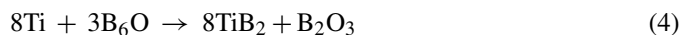


Fig. 6. SEM micrograph of sample 5-TiH<sub>2</sub> showing the TiB<sub>2</sub> precipitates (white phase) and the oxide grain boundary partially polished out.

of other oxides or TiH<sub>2</sub> which interact with B<sub>6</sub>O forming B<sub>2</sub>O<sub>3</sub>. It has to be mentioned that even the addition of an oxide free metal (TiH<sub>2</sub>) results in an increased content of B<sub>2</sub>O<sub>3</sub> due to reaction



These interactions result in an increase of B<sub>2</sub>O<sub>3</sub> in the grain boundary phase. Higher B containing glasses are softer and chemically less stable.<sup>11</sup> Therefore, they will be more sensitive to polishing than the more stable Y<sub>2</sub>O<sub>3</sub>–Al<sub>2</sub>O<sub>3</sub>–B<sub>2</sub>O<sub>3</sub> glasses generated in the case of sample 1 and 5-TiB<sub>2</sub>.

The kind of the transition metal additive (Ti, Zr, Ta, W, . . .), i.e. oxide, metal or boride has no influence on the phase formed. It has an influence only on the oxygen content of the material. Perhaps the addition of these oxides increases the oxygen content in the B<sub>6</sub>O<sub>1-x</sub>. During sintering a small shift of the lattice parameter was observed which perhaps is caused by this process. On the other hand the increase in the oxygen content can result in the formation of B<sub>2</sub>O<sub>3</sub> which forms with other oxides (Al<sub>2</sub>O<sub>3</sub>, MgO) a weak grain boundary phase or evaporates during sintering. This effect can be minimised by simultaneous addition of a transition metal or

Table 2  
Schematic presentation of the influence of the additives on the phase composition and oxygen balance in the materials.

Nr.	Addition	Phases formed during densification	Effect on composition
1	M (metal) M = Ta, W, Mo, Fe, Cr, Ni . . .	Boride	Increase of oxygen activity reducing $x$ in $B_6O_{1-x}$ or producing $B_2O_3$ , which may partially evaporate
2	$MO_x$ (metal oxide) M = Ta, W, Mo, Fe, Cr, Ni, Co	Boride	As in Nr. 1, but stronger shift to the oxygen rich compounds
3	$MB_x$ (metal boride) M = Ta, W, Mo, Fe, Cr, Ni, Co	Boride	No or minor change on the ratio of $B_2O_3/B_6O$ or the stoichiometry of $B_6O_{1-x}$
4	$M^{II}O_x$ (metal oxide) $M^{II}$ = Al, Y, Sc, Mg, Si	Borates or borate glasses, or oxides	No change in the oxygen balance, formation of an chemical stable less $B_2O_3$ rich oxide grain boundary phase

its metal oxide and elemental boron as shown in the material B-TiO<sub>2</sub>.

In contrast to the above, the addition of stable oxides like Al<sub>2</sub>O<sub>3</sub>, MgO, Y<sub>2</sub>O<sub>3</sub>, Sc<sub>2</sub>O<sub>3</sub> or their mixtures results in the stabilisation of the B<sub>2</sub>O<sub>3</sub> already present in the starting powder. Also this would minimize the reduction of the oxygen content in the B<sub>6</sub>O phase. These processes are summarized in Table 2.

#### 4. Conclusions

Based on thermodynamic considerations the use of sintering additives for boron suboxide was discussed. Two groups of materials were considered suitable for the densification:

- Oxides or metals of the transition metals of the fourth to the eighth group of the periodic table, which form borides with B<sub>6</sub>O.
- Oxides of the first to fourth main group of the periodic table and the rare earth (Sc, Y, La, and lanthanides) which, in their oxide form, are in equilibrium with B<sub>6</sub>O and form a liquid phase during densification at 1700–1900 °C.

The effectiveness of the additives was proven by means of densification experiments using the FAST/SPS method. Completely dense materials were produced with hardness ( $H_V$  0.4) higher than 33 GPa.

The addition of ZrO<sub>2</sub>, TiO<sub>2</sub>, WO<sub>3</sub> and HfO<sub>2</sub> results in the formation of the corresponding borides. Beside the boride an amorphous grain boundary phase was formed, which includes MgO, Al<sub>2</sub>O<sub>3</sub> and Y<sub>2</sub>O<sub>3</sub> if such additives were introduced. The addition of Y<sub>2</sub>O<sub>3</sub>/Al<sub>2</sub>O<sub>3</sub> results in dense materials with a minor oxide grain boundary phase indicating the stability of these oxides in contact with B<sub>6</sub>O.

It could also be shown that B<sub>6</sub>O/TiB<sub>2</sub> composites can be produced by reaction sintering of TiO<sub>2</sub> and B.

The results show that it is possible to produce dense superhard B<sub>6</sub>O materials without high pressure. The improved densification of the materials in comparison to pure B<sub>6</sub>O is connected with the formation of a liquid phase during densification. The correlation of preparation, microstructure and

properties of this new class of superhard materials needs further investigation.

#### Acknowledgment

The authors acknowledge Element Six for financial support of the research.

#### References

1. He, D., Zhao, Y., Daemen, L., Qian, J., Shen, T. D. and Zerda, T. W., Boron suboxide: as hard as cubic boron nitride. *Appl. Phys. Lett.*, 2002, **81**, 643–645.
2. Nieto-Sanz, D., Loubeyre, P., Crichton, W. and Mezouar, M., X-ray study of the synthesis of boron oxides at high pressure: phase diagram and equation of state. *Phys. Rev. B*, 2004, **70**(21), 214108 6.
3. Itoh, H., Maekawa, I. and Iwahara, H., High pressure sintering of B<sub>6</sub>O powder and properties of the sintered compact. *J. Soc. Mater. Sci. Jpn.*, 1998, **47**, 1000–1005.
4. Hubert, H., Garvie, L. A. J., Devouard, B., Buseck, P. R., Petuskey, W. T. and McMillan, P. F., High-pressure, high-temperature synthesis and characterization of boron suboxide (B<sub>6</sub>O). *Chem. Mater.*, 1998, **10**, 1530–1537.
5. McMillan, P. F., Hubert, H., Chizmeshya, A. and Petuskey, W. T., Nucleation and growth of icosahedral boron suboxide clusters at high pressure. *J. Solid State Chem.*, 1999, **147**, 281–289.
6. Sasai, R., Fukatsu, H., Kojima, T. and Itoh, H., High pressure consolidation of B<sub>6</sub>O-diamond mixtures. *J. Mater. Sci.*, 2001, **36**, 5339–5343.
7. Itoh, H., Maekawa, I. and Iwahara, H., Microstructure and mechanical properties of B<sub>6</sub>O–B<sub>4</sub>C sintered composites prepared under high pressure. *J. Mater. Sci.*, 2000, **35**, 693–698.
8. Itoh, H., Yamamoto, R. and Iwahara, H., B<sub>6</sub>O-c-BN composite prepared by high pressure sintering. *J. Am. Ceram. Soc.*, 2000, **83**, 501–506.
9. Ellison-Hayashi, C., Zandi, M., Murray, M., Csillag, F. J. and Kuo, S., Boron suboxide material and method for its preparation. US Patent 5,135,895, 1992.
10. Goosey, B. F. and Anderson, S. C., Method of fabricating boron suboxide articles. US Patent 3,816,586, 1974.
11. Brodhag, C. and Thévenot, C. F., Hot pressing of boron suboxide B<sub>12</sub>O<sub>2</sub>. *J. Less Comm. Met.*, 1986, **110**, 1–6.
12. Shabalala, T. C., McLachlan, D. S., Sigalas, I. J. and Herrmann, M., Hard and tough boron suboxide based composite. *Ceram. Int.*, 2008, **34**, 1713–1717.
13. Andrews, A., Herrmann, M., Shabalala, T. C. and Sigalas, I., Liquid phase assisted hot pressing of boron suboxide materials. *J. Eur. Ceram. Soc.*, 2008, **28**, 1613–1621.
14. Kleebe, H.-J., Lauterbach, S., Shabalala, T. C., Herrmann, M. and Sigalas, I. J., B<sub>6</sub>O: a correlation between mechanical properties and microstructure

- evolution upon  $\text{Al}_2\text{O}_3$  addition during hot-pressing. *J. Am. Ceram. Soc.*, 2008, **91**, 569–575.
15. FACTSAGE, Database Version 5.5.
  16. Andrews, A., Development of boron suboxide composites with improved toughness PhD, thesis, University of the Witwatersrand, 2008.
  17. ACerS-NIST Phase Equilibrium Diagrams, CD-ROM Database Version 3.1. Fig 06456, 02356.
  18. Telle, R., Boride-based hard materials. In *Handbook of Ceramic Hard Materials*, vol. 2, ed. R. Riedel. WILEY-VCH, 2000. pp. 803–945.
  19. Nemkovich, I. K. and Levchenya, A. A., *Steklo, Sitaly i Silikatnye Materialy. Minsk*, 1976, **5**, 69.
  20. Makarov, V. S. and Ugai, Y. A., Thermochemical study of boron suboxide  $\text{B}_6\text{O}$ . *J. Less Common. Met.*, 1986, **117**, 277–281.